Hindawi Publishing Corporation
Indian Journal of Materials Science
Volume 2015, Article ID 601827, 16 pages
http://dx.doi.org/10.1155/2015/601827

*Review Article*

# Influencing Parameters in the Photocatalytic Degradation of Organic Effluent via Nanometal Oxide Catalyst: A Review

**A. Gnanaprakasam, V. M. Sivakumar, and M. Thirumarimurugan**

*Department of Chemical Engineering, Coimbatore Institute of Technology, Coimbatore 641 014, India*

Correspondence should be addressed to V. M. Sivakumar; vmsivakumar@gmail.com

Received 26 May 2015; Accepted 2 September 2015

Academic Editor: Kourosh Kalantar-Zadeh



This paper aims to review the recent works on the photocatalytic degradation of organic pollutants in the presence of nanophotocatalyst. In this regard the effects of operation parameters which could influence the photocatalytic degradation of organic pollutants (such as catalyst preparation method, initial concentration of organic pollutants, presence of doping, catalyst loading, calcinations temperature, pH, presence of oxidants, UV intensity, temperature, and presence of supports) are discussed. Recent research suggests that the parameters mentioned above have great influence on the photocatalytic activity of prepared nanocatalyst. Also, the general mechanism of photocatalytic degradation and some recent synthesis methods are discussed here.

## 1. Introduction

In recent years development of industries like textile, leather, paint, food, plastics, and cosmetics is enlarged and these industries are connected with the discarding of a vast number of organic pollutants which are harmful to microbes, aquatic system, and human health by influencing the following parameters [1–4]. In addition to that the effect of these organic effluents in the wastewater can be sensed by change in the vital parameters of the discharged water such as chemical oxygen demand, biochemical oxygen demand, toxicity, unpleasant odour, and colour [5]. Even the presence of a trace amount of colored organic compounds in the aquatic system can result in coloration of wastewater. The consequence of colored water is detrimental to environment since the color obstructs the sunlight access to aquatic organisms and plants, and it diminishes the photo synthesis and affects the ecosystem [6, 7]. Therefore, the removal of color and sanitization have become an ecological concern and they are vital for the environmental sustainability. Industrial development and its association with discharge of organic matter into the aquatic systems demands the technological development to solve the environmental problems related to organic effluents [8]. Many practices have been widely applied in the treatment of organic effluent such as biological treatment, reverse osmosis, ozonation, filtration, adsorption on solid phases, incineration, and coagulation [9]. However, each of the methodologies has its own advantages and limitations; as such incineration can result in deadly toxic volatiles products [10]; biological treatment needs prolonged treatment time and results in ghastly smell; ozonation can be effective way for the treatment of organic effluent but the stability of ozone is the biggest concern which was well influenced by the existence of salts, pH, and temperature [9, 11]. The traditional physical methods (adsorption, filtration, reverse osmosis and coagulation) are quite expensive and also these techniques do not eliminate the organic molecules utterly but just transform one phase to another [12, 13]. In recent era, advanced oxidation processes (AOPs) have been found as an effective and alternative way for the treatment of organic effluent in aqueous system [14–16]. The recent research demonstrates that AOPs based on photocatalysts are valuable and this method benefits complete mineralization of organic molecules into nontoxic $CO_2$ and $H_2O$ at the atmospheric conditions [17–20]. Further, AOPs result in the generation of hydroxyl radicals ($^{\bullet}OH$) as main oxidizing agents which can remove even nonbiodegradable organic compounds from wastewater stream [21, 22]. Photocatalytic degradation of organic effluent

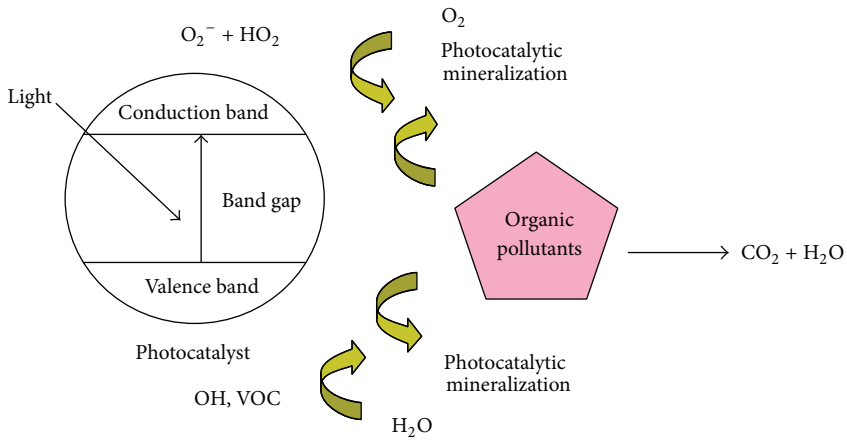


Figure 1: Schematic diagram of photocatalytic degradation of organic effluent.

emerged as one of the best methodologies for the treatment of toxic organic effluents which uses the semiconductor as catalyst such $TiO_2$, ZnO, ZnS, $WO_3$, CdS and $Fe_2O_3$, and $SrTiO_3$ [23, 24, 24–27]. Among them $TiO_2$ and ZnO have been widely applied as photocatalyst due to their high activity, nontoxicity, chemical stability, lower costs, optical and electrical properties, and environment friendly characteristics [28–32]. Since the first revolutionary papers in the 1970s, the attention of researchers in heterogeneous photocatalyst has developed greatly [33, 34] and showed the advantages of photocatalytic practices over the conventional techniques, such as rapid oxidation, no formation of polycyclic compounds, complete oxidation of pollutants, and high efficiency [35–37]. In this manner, the heterogeneous photocatalyst turns out to be an elegant alternative for organic effluent treatment and the catalyst reduced to the nanoscale can demonstrate different properties compared to properties at macroscale size, facilitating unique applications in photocatalyst degradation of organic waste [38]. Nanophotocatalysts have been intensively examined because of their increased surface area which sturdily influences their physiochemical properties [39, 40]. Efficiency of the prepared photocatalyst for the degradation of organic effluent is greatly influenced by various parameters, starting from synthesis of nanocatalyst to operation condition of degradation of effluent. In recent year nanocatalyst synthesis and its application in the degradation of organic molecules were studied extensively [41]. This paper discusses the various factors which could affect the photocatalytic activity of the nanocatalyst staring from synthesis of operating condition.

## 2. Reaction Mechanism

In general, the photocatalytic degradation involves several steps such as adsorption-desorption, electron-hole pair production, recombination of electron pair, and chemical reaction [42, 43]. The general mechanism of photocatalytic degradation of organic molecules is explained as follows (Figure 1): [39, 44–46]. When the photocatalyst (PC) is irradiated with photons of energy equal to or more than band gap energy of PC, the electrons ($e^-$) are excited from the valence band (VB) to the conduction band (CB) with the simultaneous creation of holes ($h^+$) in the VB:

$$PC + hv \longrightarrow e_{CB}^- + h_{VB}^+ \quad (1)$$

where $h_V$ is the energy essential to transfer the electron from valence band to conduction band. The electrons generated through irradiation could be readily trapped by $O_2$ absorbed on the photocatalyst surface or the dissolved $O_2$ to give superoxide radicals ($O_2^{\bullet -}$):

$$e_{CB}^- + O_2 \longrightarrow O_2^{\bullet -} \quad (2)$$

Consequently, $O_2^{\bullet -}$ could react with $H_2O$ to produce hydroperoxy radical ($HO_2^\bullet$) and hydroxyl radical ($OH^\bullet$), which are strong oxidizing agents to decompose the organic molecule:

$$O_2^{\bullet -} + H_2O \longrightarrow HO_2^\bullet + OH \quad (3)$$

Simultaneously, the photoinduced holes could be trapped by surface hydroxyl groups (or $H_2O$) on the photocatalyst surface to give hydroxyl radicals ($OH^\bullet$):

$$h_{VB}^+ + OH^- \longrightarrow {}^\bullet OH_{ad}$$
$$h_{VB}^+ + H_2O \longrightarrow {}^\bullet OH + H^+ \quad (4)$$

Finally the organic molecules will be oxidized to yield carbon dioxide and water as follows:

$$^\bullet OH + \text{organic molecules} + O_2 \longrightarrow \text{products}\,(CO_2 \text{ and } H_2O) \quad (5)$$

Meanwhile, recombination of positive hole and electron could take place which could reduce the photocatalytic activity of prepared nanocatalyst:

$$e_{CB}^- + h_{VB}^+ \longrightarrow PC \quad (6)$$

## 3. Nanocatalyst Preparation Methods

Here some of the recently used methods for the preparation of nanocatalyst in the photocatalytic application are discussed briefly.

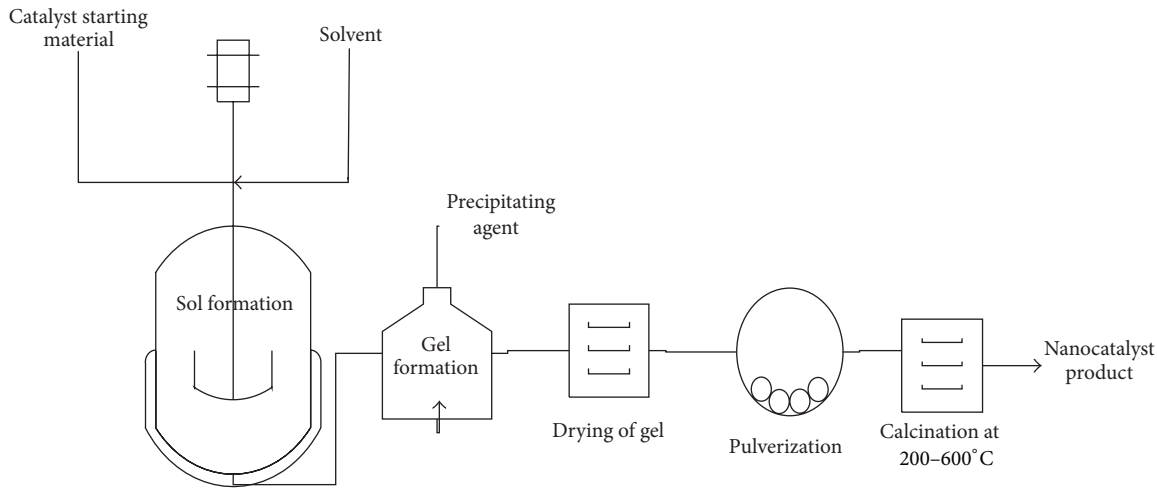


Figure 2: Synthesis of photo nanocatalyst by sol-gel method.

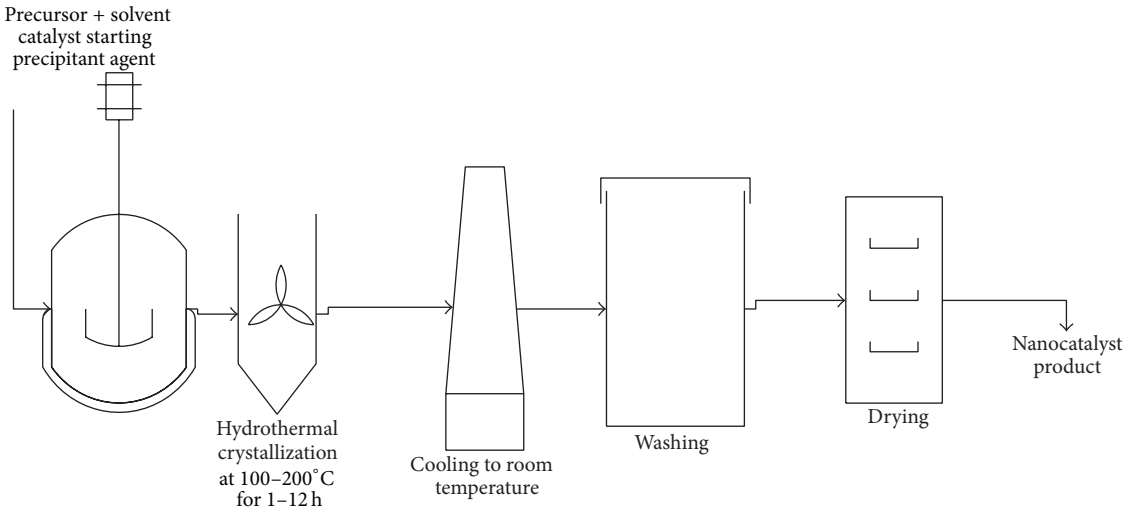


Figure 3: Synthesis of photo nanocatalyst by hydrothermal treatment method.

*3.1. Sol-Gel Method.* Synthesis of photo nanocatalyst by sol-gel method is shown in Figure 2.

Catalyst starting material is dissolved in the suitable solvent and then precipitating agent is added dropwise with vigorous stirring and solvent and precipitate (gel) are separated. To eliminate even the trace amount of the solvents in the obtained gel, the gel has to be dried at temperature between slightly near and above the boiling point of solvent; then product is pulverized and calcined to get the desired nanocatalyst [63, 64].

*3.2. Hydrothermal Method.* Synthesis of photo nanocatalyst by hydrothermal treatment method is shown in Figure 3.

In hydrothermal treatment method, precursor is dissolved in the solvent. Then, the precipitating agent is added dropwise followed by hydrothermal treatment of prepared solution at 100–200°C for 1–12 hours in autoclave under autogenous pressure. The solid particles are cooled and washed with washing agent and then dried for 24 h at 80°C to give nanoparticles [65, 66].

*3.3. Coprecipitation Method.* Synthesis of photo nanocatalyst by coprecipitation method is shown in Figure 4.

Precursor of catalyst and doping agent are dissolved separately in deionized water and mixed under vigorous stirring to get the uniform distribution of dissolved materials. Then, precipitating agent (NaOH) was added dropwise into precursor solution with the continuous stirring of the particular period of time. The precipitate is filtered and washed with deionised water until the washed solution reaches neutral pH. The obtained precipitate is dried at 80–100°C in an oven for 24 h and calcined at 400–500°C for 5 h to get the nanocatalyst [65, 67].

*3.4. Reverse Microemulsion Method.* Synthesis of photo-nanocatalyst particle by reverse microemulsion method is shown in Figure 5.

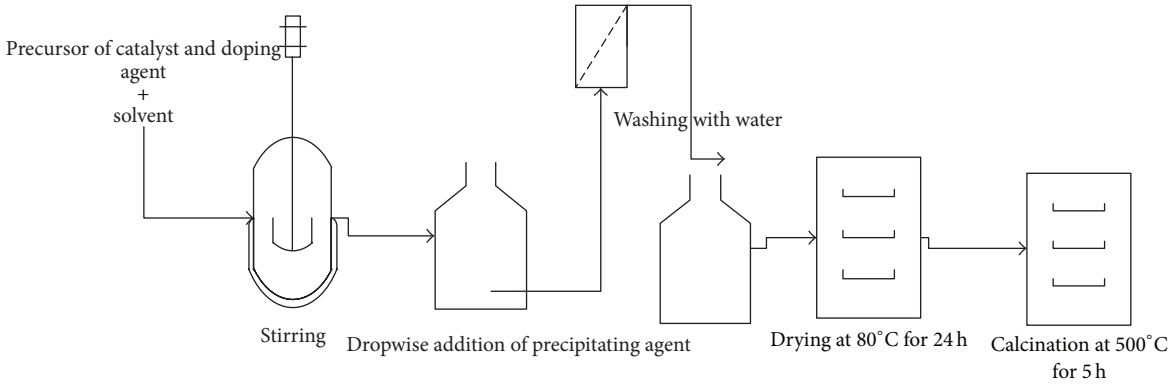


Figure 4: Synthesis of photo nanocatalyst by coprecipitation method.

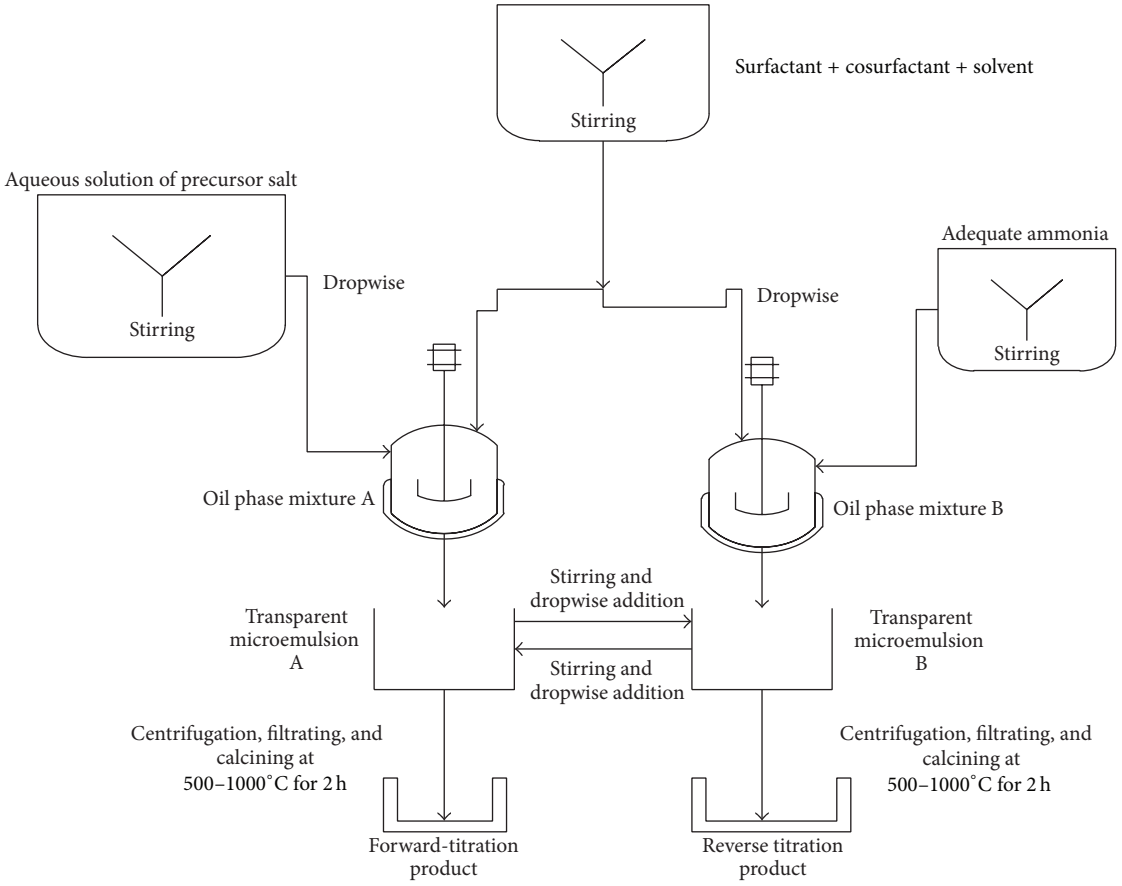


Figure 5: Synthesis of photo nanocatalyst particle by reverse microemulsion method.

Desired mole ratios of precursor salts are dissolved in the deionized water. The surfactant and cosurfactant are mixed in solvent with vigorous stirring. As shown in Figure 5, two types of microemulsions are prepared. In part A, mixture of aqueous solution of precursor salts is added into one of the mixtures of surfactant and cosurfactant to result in transparent microemulsion A. In the same manner, the adequate ammonia is added into the other microemulsion mixture to yield a transparent microemulsion B (part B). Then parts A and B are mixed continuously until clear solution appeared and solution was allowed 1-2-day aging. Subsequently, after centrifugation, washing, drying, and calcinations of separated particles could be done to yield the effective photocatalyst [68].

## 4. Factor Affecting the Photodegradation

*4.1. Nanocatalyst Preparation Method/Condition.* In general, changes in process conditions or preparation methods result in catalyst with different catalytic activity. In recent decades,

Table 1: Comparison of photocatalytic activity of nanocatalyst at different initial pollutant concentration.

| Light source | Catalyst preparation method | Catalyst used | Organic pollutant | Initial pollutant concentration | Irradiation time (min) | Degradation efficiency (%) | Reference |
|---|---|---|---|---|---|---|---|
| Solar radiation | Sol-gel method | $TiO_2$ | 2-Chlorophenol | 50 mg/lit | 90 | 100 | [47] |
| | | | | 100 mg/lit | 120 | 100 | |
| | | | | 150 mg/lit | 120 | 100 | |
| Solar radiation | Sol-gel method | $TiO_2$ | 2,4-Dichlorophenol | 50 mg/lit | 100 | 100 | [47] |
| | | | | 100 mg/lit | 120 | 100 | |
| | | | | 150 mg/lit | 120 | 100 | |
| Solar radiation | Sol-gel method | $TiO_2$ | 2,4,6-Trichlorophenol | 50 mg/lit | 120 | 100 | [47] |
| | | | | 100 mg/lit | 120 | 100 | |
| | | | | 150 mg/lit | 120 | 100 | |
| 100 W mercury lamp | Sol-gel method | Codoped $TiO_2$ | 2-Chlorophenol | 12.5 ppm | 180 | 100 | [48] |
| | | | | 25 ppm | | 95 | |
| | | | | 50 ppm | | 90 | |
| | | | | 75 ppm | | 80 | |
| UV radiation | P25 | $TiO_2$ | Victoria blue R | 0.5 g/L | 720 | 100 | [49] |
| | | | | 1.5 g/L | | 50 | |
| | | | | 2.5 g/L | | 30 | |

there are many researchers who has been involved in the modification of catalyst preparation method to improve the photocatalytic activity of prepared nanocatalyst [69, 70]. For example, in the case of $TiO_2$ catalyst, it was found that lab-made rutile exhibited a good photocatalytic activity due to presence of vast number of hydroxyl groups (Table 4). But contradictory to that the rutile obtained at a higher temperature is inactive due to limited surface hydroxyl content [66]. Further, many researchers have observed that size of the prepared catalyst is very well influenced by condition of catalyst preparation [71]. It is desired to have photocatalyst with smaller size to result in a higher photocatalytic activity. But reduction in the size of photocatalyst leads to increase in surface energy of the photocatalyst. This causes the agglomeration of particles which could reduce the porosity of the catalyst. Thereby access of organic molecules could be prevented into interparticle porous surface and reduce the surface area available. It obliterates photocatalytic activity of prepared photocatalyst [72]. But the above could be eliminated by doing slight change in sol-gel method by using stearic acid as capping agent to prevent agglomeration of small size nanoparticles due to surface repulsion [73, 74]. By using surfactant as electrostatic stabilization agent, calcination temperature required for the formation of anatase phase $TiO_2$ could be reduced [75]. And, it was found that deposition of dopant ions on the surface of photocatalyst is well affected by the pH of precursor solution [76].

*4.2. Initial Concentration of Organic Compound.* Increasing initial organic compound concentration reduces the photocatalyst degradation efficiency. It might be due to the increase of the initial concentration of organic compound in which more molecules were adsorbed on the surface of the photocatalyst. This results in unavailability of catalyst surface for the building of hydroxyl radicals which reduces the photocatalytic activity of the catalyst [49]. Also, escalating initial concentration of organic compound decreases the number of photons or path length of photon that is arrived on the surface of photocatalysis (the Beer-Lambert law) which reduces the excitation of electron from valance band to conduction band. It results in the decrease in the photocatalytic activity of prepared nanocatalyst [18, 30, 50, 77]. Comparison of removal percentage of organic pollutants at different initial pollutant concentration is presented in Table 1.

*4.3. Doping.* Doping of photocatalyst could improve the photocatalyst efficiency in the following way: (1) band gap narrowing [67]; (2) formation impurity energy levels [78]; (3) oxygen vacancies; (4) unique surface area for the adsorption of organic molecules [79]; and (5) electron trapping [39]. In general catalyst with a smaller band gap energy is preferred to be an effective photocatalyst to generate more electron-hole pairs [72]. Band gap narrowing, introduction of impurity energy level, and oxygen-deficient sites can result in a catalyst with higher photocatalytic activity even under visible light [63, 78, 80–83]. The photocatalytic activity of prepared catalyst depend well on how the recombination of photoinduced hole-electron pairs is prevented. Doping prevents recombination of electrons and holes and gets better the photocatalytic activity by trapping the photoinduced electrons [28, 30, 46, 84, 85]. Incorporation of dopant ions in the catalyst is either interstitial or substitutional. In the case of interstitial mode, the radius of doped ions will be lesser than the radius of lattice ions and the lattice space. This allows the doped ions to pierce the crystal cell of the metal oxide. In the case of substitutional mode, doping ions replace the lattice oxide or lattice ions [78]. Further, it has been found that the dopant ions incorporated into catalyst crystal lattice can alter the electronic property

Table 2: Comparison of photocatalytic activity of $TiO_2$ with different noble metal doping.

| Doping and optimum doping concentration (wt %) | Light source | Catalyst preparation method | Catalyst used | Organic pollutant | Irradiation time (min) | Degradation efficiency (%) | Reference |
|---|---|---|---|---|---|---|---|
| 1.5 | UV radiation | Photochemical reduction | Pt doped $TiO_2$ | Methyl orange | 90 | 98 | [14] |
| 3 | UV radiation | Photo reduction | Ag doped $TiO_2$ | Direct red 23 | 120 | 97 | [50] |
| 0.8 | UV radiation | Impregnation | Au doped $TiO_2$ | Acid green 16 | 60 | 98 | [51] |

Table 3: Comparison of photocatalytic activity of different metal doped photocatalyst.

| Doping and optimum doping concentration (mol %) | Light source | Catalyst preparation method | Catalyst used | Organic pollutant | Irradiation time | Degradation efficiency (%) | Reference |
|---|---|---|---|---|---|---|---|
| 0.50 | UV radiation | FSP technique | Nb-loaded ZnO | Phenol | 18.40 min | 100 | [52] |
| 0.1 | UV radiation | Combustion technique | Codoped $TiO_2$ | Phenol | 45 min | 100 | [53] |
| 0.02 | 500 W halogen lamp | Coprecipitation method | Ni-doped ZnS | Methylene blue | 120 min | 50 | [54] |
| 0.036 | 100 W mercury lamp | Sol-gel method | Codoped $TiO_2$ | 2-Chlorophenol | 180 min | 90% | [48] |

of prepared nanocatalyst and improve its light absorption ability in the visible light region [1, 18, 78]. It has been found that the red-shift of absorption edge with respect to pure material is resulted from d electron transfer. But beyond optimum level of doping concentration decrease in photocatalytic activity results from (i) decreasing surface area of catalyst and (ii) narrowing space charge region, and the penetration depth of radiation into photocatalyst may exceed the space charge layer, so that the recombination of the photogenerated hole-electron pairs turns to be easier [86], and some case doping particles can act as electron-hole recombination centres [28, 50, 87], because the average distance between trap sites is reduced with increasing the dopant concentration [74]. Thus the photocatalytic activity of nanocatalyst is decreased. Tian et al. found that, in the case of $TiO_2$, the composition of rutile is increased to some extent with increasing doping concentration by reducing the thermal stability of anatase and favours the phase transformation from anatase to rutile [1]. In addition to that, the increase in the doping content results in clusters of doping molecule to form overlying agglomerates which can shadow the photocatalytic activity by surface plasmon absorption phenomenon [46]. In the case of mesoporous nanoparticles, doping material might be ascribed to lower photocatalytic activities due to the fact that surface site might be blocked by doping material [88, 89]. In contrast to that, Tong et al. reported that doping increases the surface area by increasing mesoporous structure in the nanocatalyst [90].

*4.3.1. Noble Metal Doping.* Noble metal may enhance photocatalytic activity through the following route: (i) enhanced adsorption of organic molecules on the photocatalyst surface [40], (ii) the surface plasmon resonance of noble nanoparticles on photocatalyst which is excited by visible light, increasing electron excitation and electron-hole separation [91], (iii) noble nanoparticles acting as electron traps to hinder electron/hole recombination [54], and (iv) Fermi level equilibration between noble nanoparticles and photocatalyst (semiconductors) which may lessen the band gap of the photocatalyst and in turn weaken the fast electron-hole pairs recombination [40], and also it is reported that the photo corrosion of ZnO catalyst is prevented by adding pt doping to the photocatalyst. Thereby life time of catalyst is increased [85].

Comparison of the photocatalytic degradation rate of different organic pollutants for different noble metal doping is given in Table 2.

*4.3.2. Metal Doping.* Metal doping could alter the morphology, particle size [89], crystal structure [27], and specific surface area of nanocatalyst which are significant factors that decide the photocatalytic activity of prepared photocatalyst.

Comparison of photocatalytic activity of different metal doped catalyst is presented in Table 3.

*4.3.3. Nonmetallic.* Anionic dopants are reported to be superior than metal dopants regarding stability of the doped photocatalyst, photocatalytic activity, and simplicity of doping process [92]. The quantum yield of doped photocatalyst under visible light irradiation is far lower than that of photocatalyst under UV irradiation. Photocatalyst with anion-doping to obtain the visible light-activated photocatalyst has been reported in last decades [42, 62, 79, 93, 94]. Various anionic species such as nitrogen, carbon [95], phosphorus, fluorine [96], and sulphur were recognized to potentially form a new impurity energy level neighboring to the valence band while maintaining the largest band gap for maximum efficiency. Nitrogen can be incorporated into the nanophotocatalyst structure as substitutional and as interstitials [42]. In the case of activated carbon hybridized nanophotocatalyst, the surface area of photocatalyst increases with the increase

Table 4: Photocatalytic activity of nonmetallic doped $TiO_2$ catalyst.

| Optimum doping concentration (% wt) | Light source | Catalyst preparation method | Catalyst used | Organic pollutant | Irradiation time (min) | Degradation efficiency (%) | Reference |
|---|---|---|---|---|---|---|---|
| 0.012 | UV radiation | Hydrothermal | S doped $TiO_2$ | Methyl orange | 42 | 96 | [55] |

Table 5: Photocatalytic activity of earth metal doped photocatalyst.

| Doping and optimum doping concentration | Light source | Catalyst preparation method | Catalyst used | Organic pollutant | Irradiation time (min) | Degradation efficiency (%) | Reference |
|---|---|---|---|---|---|---|---|
| 1.5% $Er^{3+}$ | UV radiation | Sol-gel method | $Er^{3+}$ doped $TiO_2$ | Orange I | 60 | 100 | [56] |

in activated carbon content but activity decreases due to increase of $ZnO/TiO_2$ concentration, because the pore entrances of the activated carbon could be blocked by excess $ZnO/TiO_2$ composition [62, 96]. Also Yu et al. found that the crystalline nature of prepared catalyst was suppressed by the increase in the amount of doping with cerium and nitrogen, and this trend was strengthened with the increase in doping amount. Meanwhile, the growth of crystal size of catalyst was suppressed to different extent of doping [87].

*4.3.4. Earth Metals Doping.* In case of $TiO_2$ nanocatalyst preparation, phase transition from anatase to rutile was inhibited by earth ions during the thermal treatment. Similar result is observed in nonmetal dopant and combination of nonearth and nonmetal dopants [79, 89]. In the case of $TiO_2$, the inhibition of the phase transition was ascribed to the stabilization of the anatase phase by rare earth ions through the formation of $TiO_2$ rare earth element bonds [64]. Rare earth metal doping significantly inhibits the growth of nanocrystalline size [64, 97] due to earth metal-O-Ti bonds formation on the surface of nanocatalyst and in the calcinations [56, 64, 98]. Shi et al. [64] observed that unit cell volumes and lattice distortion of doped nanocatalyst particles are larger than that of undoped photocatalyst, because small part of Ti ions are replaced by earth metal ions in the $TiO_2$ lattice, and this causes the distortion and expansion of lattice crystal structure. Similar result has been reported for $Fe^{3+}$ doping [90]. It results in easy absorption of oxygen molecules as electron trap on the defects which originated from the lattice distortion and expansion. Therefore the recombination rate of electron-hole pairs could be decreased and increased photocatalytic activity of the nanocatalyst is observed. Photocatalytic activity of earth metal doped photocatalyst is given in Table 5.

*4.4. Catalyst Loading.* In general due to increasing in active sites, the rate of photocatalytic degradation organic pollutants increases with photocatalyst dosage [6, 32, 60]. This is mainly due to increase of hydroxyl radical produced from irradiated photocatalyst [46, 99]. At lower catalyst loading, degradation of organic molecule is low, because more light is transmitted through the reactor and lesser transmitted radiation only will be utilised in the photocatalytic reaction [49, 61]. But beyond the optimum amount of catalyst loading, the degradation rate might be reduced due to increase in the opacity of the suspension, and thus increasing the light scattering and also the infiltration depth of the photons is diminished and less photocatalysts could be activated [18, 84, 100]. Additional to what is mentioned above, agglomeration of nanoparticles at high concentrations reasoning a decline in the number of surface active sites available for the photocatalytic degradation [77, 99] and deactivation of activated molecules could result from the collision of activated molecules with ground state molecules [61, 101]. Dependence of photocatalytic activity on catalyst loading is given in Table 6.

*4.5. Calcination Temperature.* Calcination temperature has a vital influence on the optical property, crystal size, and crystal structure of the prepared photocatalyst [56]. Moreover, the common synthesis of nanophotocatalyst usually involves high-temperature calcinations to translate amorphous into crystal structure, which usually results in particle growth and leads to decrease in surface area and decrease in photocatalytic degradation efficiency [64, 75, 101]. Shi et al. reported [64] that the absorption profile shifted slightly to longer wavelengths (red-shift) with the increase of calcined temperature. In the case of $TiO_2$, anatase phase has higher thermal stability than rutile phase which results in higher concentration of anatase phase at higher temperature [1], and it has been reported that anatase possesses higher photocatalytic activity than rutile [64, 102]. Because the adsorptive affinity of anatase for organic molecules is higher than that of rutile, anatase structure also displays low rate of recombination of hole-electron pair in contrast to rutile [64], and also higher calcination temperature helps the formation of larger crystals and the rutile phase by agglomeration [74], Sun et al. found that doping of nitrogen with $TiO_2$ would drop increasingly with rise in temperature and the crystal particle sizes of doped photocatalyst became bigger with increasing calcinations temperature [103]. Comparison of photocatalytic degradation of different organic pollutants for different calcinations temperature is shown in Table 7.

*4.6. pH.* pH of aqueous dye solution plays a vital role in the photocatalytic activity of prepared catalyst. pH influences the adsorption and dissociation of the organic molecule [41, 104], surface charge of photocatalyst, and oxidation potential of the valence band [101]. Photocatalyst surface is predominantly negatively charged when the pH is increased beyond isoelectric point of nanophotocatalyst. As the pH reduced, the functional groups are protonated, thus raising the positive charge of photocatalyst surface. The surface of

Table 6: Dependence of photocatalytic activity on catalyst loading.

| Source of catalyst | Light source | Catalyst preparation method | Catalyst used | Organic pollutant | Catalyst concentration | Irradiation time | Degradation efficiency (%) | Reference |
|---|---|---|---|---|---|---|---|---|
| $TiCl_4$ and cobalt(III) 2,4-pentanedionate | UV radiation | Sol-gel method | Codoped $TiO_2$ | 2-Chlorophenol | 10 mg/L | 3 h | 96.4 | [57] |
| | 100 W mercury lamp | Sol-gel method | Codoped $TiO_2$ | 2-Chlorophenol | No catalyst | 180 min | 10 | [48] |
| | | | | | 5 | | 50 | |
| | | | | | 10 | | 90 | |
| | | | | | 30 | | 90 | |

Table 7: Comparison of photocatalytic degradation of different organic pollutants for different calcinations temperature.

| Light source | Catalyst preparation method | Catalyst used | Catalyst dosage | Organic pollutant | Calcinations temperature (°C) | Irradiation time | Degradation efficiency (%) | Reference |
|---|---|---|---|---|---|---|---|---|
| UV radiation | Sol-gel technique | $TiO_2$ | 2.5 mg/lit | Phthalic acid | 673 | 475 min | 99 | [58] |
| | | | | | 723 | | 45 | |
| 100 W mercury lamp | Sol-gel method | Codoped $TiO_2$ | 10 mg/lit | 2-Chlorophenol | 100 | 180 min | 30 | [48] |
| | | | | | 400 | | 50 | |
| | | | | | 600 | | 90 | |
| | | | | | 800 | | 60 | |

Table 8: Optimum pH for the different photocatalytic system.

| Light source | Catalyst preparation method | Initial concentration | Catalyst used | Organic pollutant | Optimum pH | Irradiation time (min) | Degradation efficiency | Reference |
|---|---|---|---|---|---|---|---|---|
| UV light | Hydrothermal process | 2000 mg/lit (COD) | $TiO_2$ | Coking water | 7 | 60 | 30% | [59] |
| 100 W mercury lamp | Sol-gel method | 50 ppm | Codoped $TiO_2$ | 2-Chlorophenol | 12 | 180 | 95% | [48] |
| UV light | Degussa P25 | $1.2 \times 10^{-4}$ M | $TiO_2$ and cement | Reactive yellow dye 17 | 5–7 | 480 | 85 | [60] |
| 40 W fluorescent lamp | Aqueous reaction method | $6 \times 10^{-6}$ M | MnWO4 | Methyl orange | 9 | 480 | 50 | [41] |

Table 9: Dependence of photocatalytic activity on light intensity.

| Light source | Catalyst preparation method | Catalyst used | Organic pollutant | Initial concentration | Irradiation time (min) | Degradation efficiency | Reference |
|---|---|---|---|---|---|---|---|
| UV radiation | Hydrothermal method | $TiO_2$ | Coke water | 2000 mg/lit (COD) | 60 min | 15% (400 $mWcm^{-2}$)<br>30% (1300 $mWcm^{-2}$) | [47] |
| UV radiation<br>Sun light | Degussa P25 | $TiO_2$ | Reactive yellow 17 | $1 \times 10^{-4}$ M | 360<br>720 | 100 | [61] |
| UV radiation<br>Sun light | Simple mixing | 9AC–ZnO | 4-Acetylphenol | $3 \times 10^{-4}$ mol/$L^{-1}$ | 150<br>120 | 100 | [62] |

photocatalyst will be charged negatively and results in the increased adsorption cationic molecules at higher pH value while in the reverse situation it would adsorb anionic molecules very easily [27, 49, 50, 99]. In the meantime, the increased pH value increases the hydroxyl radicals generation [105]. But the degradation of organic molecules is repressed when the pH of solution is too high (pH > 12), because hydroxyl ions compete with organic molecules for the adsorption on the surface of the catalysts [27]. On the contrary, at low pH, the adsorption of cationic organic molecule on the photocatalyst surface is reduced, because the surface of photocatalyst is positively charged which results in the decrease in adsorption of cationic organic molecules. Thus, the degradation efficiency is declined in lower pH or acidic solution [18, 77, 106]. That is, the optimum pH of solution has to be fixed for the different organic solution.

On the other hand, Prado and Costa [107] noticed that the degradation of malachite green was lesser in basic medium (higher pH); the degradation efficiency of photocatalyst increases with the decrease in pH value. Similar effects were observed by other researchers [32, 52]. Optimum pH for the different photocatalytic system is presented in Table 8.

*4.7. Effect of Oxidants.* The electron-hole recombination in photocatalyst can be diminished by adding some irreversible electron acceptors ($H_2O_2$, $(NH_4)_2S_2O_8$, $KBrO_3$, and $K_2S_20_8$) to the reaction mixture [14, 50]. In most cases, $H_2O_2$ is used to increase the photocatalytic activity of prepared photocatalyst.

The mechanism in which $H_2O_2$ alters the photocatalytic degradation is given as follows:

$$\begin{aligned} H_2O_2 + O_2^{\bullet -} &\longrightarrow {}^{\bullet}OH + OH^- + O_2 \\ H_2O_2 + h\nu &\longrightarrow 2{}^{\bullet}OH \\ H_2O_2 + e_{CB}{}^- &\longrightarrow {}^{\bullet}OH^{+\bullet}OH^- \end{aligned} \quad (7)$$

The increase of $H_2O_2$ concentration resulted in a quicker degradation of the organic molecules [108]. Because photolysis of $H_2O_2$ is to generate OH radicals and $H_2O_2$ helps for trapping electrons and thus prevents the recombination of hole-electron pairs, in consequence, the chance of the formation of OH radical and $O_2$ on the surface of the photocatalyst is increased. Beyond the optimum concentration of $H_2O_2$, increase in $H_2O_2$ level decreases the degradation rate of dye due to quenching of OH radical by $H_2O_2$ [60]. Sobana and Swaminathan reported that addition of $H_2O_2$ beyond the optimum level results in generation of peroxide radical, which acts as a hole scavenger and thus results in the decrease of photocatalytic degradation efficiency [30].

*4.8. Light Intensity.* Semiconductor catalyst absorbs the light with an energy equal to or more than band gap energy [83] which causes the movement of electrons from valence band to conduction band by leaving holes in the valance band [36, 77]. The photocatalytic degradation rate increased with increasing intensity of radiation [59]. The chance of excitation of catalyst can be improved by raising the intensity of incident radiation [109]. But recombination of hole-electron pair is a normally encountered difficulty in photocatalysis. At lower light intensity, hole-electron pair separation struggles with recombination which reduces the formation of free radicals and, thus, causes reduction in the degradation of the organic molecules [61] which could be eliminated by using light with higher intensity. Therefore, enhancement of the photodegradation rate could be achieved with increase in the intensity of incident radiation [28, 101]. Dependence of photocatalytic activity on light intensity is presented in Table 9.

*4.9. Effect of Temperature.* The photocatalytic degradation efficiency of organic molecules steadily increased as the temperature is raised. When the temperature is increased, it causes the bubbles formation in the solution which results in the generation of free radicals. Additionally, the increase in temperature helps the degradation reaction to overcome electron-hole recombination. Besides that, the increasing temperature may enhance the oxidation rate of organic molecules at the interface [32]. Influence of reaction temperature on photocatalytic degradation is presented in Table 10.

*4.10. Effect of the Support.* Application of support for the nanophotocatalyst maintains the dispersion of the nanoparticle and prevents agglomeration and sintering [104, 110]. Also, supports increase the photocatalytic activity by enhancing charge separation (high electric conductivity supports) or the adsorption of organic molecules [19]. Generally support/magnetic coating is used to immobilize the nanocatalyst so that the reusability of nanocatalyst can be achieved [111, 112], and also supports help the adsorption of organic molecules to increase the efficiency of photocatalytic degradation. The organic pollutants, which are adsorbed on the mesoporous (support) materials, have an opportunity to be

Table 10: Comparison of the photocatalytic degradation rate of organic pollutants at different temperature.

| Light source | Catalyst preparation method | Catalyst used | Organic pollutant | Temperature | Irradiation time | Degradation efficiency (%) | Reference |
|---|---|---|---|---|---|---|---|
| UV radiation | Sol-gel method | Ag doped $TiO_3$ | Rhodamine B dye | 5°C | 180 min | 35 | [39] |
| | | | | 15°C | | 40 | |
| | | | | 25°C | | 55 | |
| | | | | 45°C | | 60 | |
| | | | | 55°C | | 63 | |

degraded due to the appearance of hydroxyl radical on the support surface [77, 113].

## 5. Conclusion

The technology of nanocatalyst as a photocatalyst has undergone an explosive growth during the past decade, for environmental remediation by using both artificial and natural UV-visible irradiation. Hence it is possible to obtain visible light-active photocatalyst achieved by altering the synthesis and operating condition, so that industrial implementation of photocatalytic degradation of organic effluent can be achieved over conventional treatment methods.

## Conflict of Interests

The authors declare that there is no conflict of interests regarding the publication of this paper.

## References

[1] B. Tian, C. Li, F. Gu, H. Jiang, Y. Hu, and J. Zhang, "Flame sprayed V-doped $TiO_2$ nanoparticles with enhanced photocatalytic activity under visible light irradiation," *Chemical Engineering Journal*, vol. 151, no. 1–3, pp. 220–227, 2009.

[2] L. M. S. Colpini and H. J. Alves, "Onélia aparecida andreo dos sant," *Dyes and Pigments*, vol. 76, pp. 525–529, 2008.

[3] T. Robinson, G. McMullan, R. Marchant, and P. Nigam, "Remediation of dyes in textile effluent: a critical review on current treatment technologies with a proposed alternative," *Bioresource Technology*, vol. 77, no. 3, pp. 247–255, 2001.

[4] R. Vinu and Giridhar, "Catalysis at interface," *Journal of the Indian Institute of Science*, vol. 90, no. 2, pp. 118–230, 2010.

[5] A. B. Dos Santos, F. J. Cervantes, and J. B. van Lier, "Review paper on current technologies for decolourisation of textile wastewaters: perspectives for anaerobic biotechnology," *Bioresource Technology*, vol. 98, no. 12, pp. 2369–2385, 2007.

[6] S. Senthilvelan, V. L. Chandraboss, B. Karthikeyan, L. Natanapatham, and M. Murugavelu, "$TiO_2$, ZnO and nanobimetallic silica catalyzed photodegradation of methyl green," *Materials Science in Semiconductor Processing*, vol. 16, no. 1, pp. 185–192, 2013.

[7] M.-S. Chiou and H.-Y. Li, "Equilibrium and kinetic modeling of adsorption of reactive dye on cross-linked chitosan beads," *Journal of Hazardous Materials*, vol. 93, no. 2, pp. 233–248, 2002.

[8] W. Zhou, M. Cao, S. Su et al., "A newly-designed polyoxometalate-based plasmonic visible-light catalyst for the photodegradation of methyl blue," *Journal of Molecular Catalysis A: Chemical*, vol. 371, pp. 70–76, 2013.

[9] J. García-Montaño, X. Domènech, J. A. García-Hortal, F. Torrades, and J. Peral, "The testing of several biological and chemical coupled treatments for Cibacron Red FN-R azo dye removal," *Journal of Hazardous Materials*, vol. 154, no. 1–3, pp. 484–490, 2008.

[10] M. Vinita, R. P. J. Dorathi, and K. Palanivelu, "Degradation of 2,4,6-trichlorophenol by photo Fenton's like method using nano heterogeneous catalytic ferric ion," *Solar Energy*, vol. 84, no. 9, pp. 1613–1618, 2010.

[11] C. C. Chen, C. S. Lu, Y. C. Chung, and J. L. Jan, "UV light induced photodegradation of malachite green on $TiO_2$ nanoparticles," *Journal of Hazardous Materials*, vol. 141, no. 3, pp. 520–528, 2007.

[12] G. Zelmanov and R. Semiat, "Phenol oxidation kinetics in water solution using iron(3)-oxide-based nano-catalysts," *Water Research*, vol. 42, no. 14, pp. 3848–3856, 2008.

[13] S. Kaur and V. Singh, "$TiO_2$ mediated photocatalytic degradation studies of Reactive Red 198 by UV irradiation," *Journal of Hazardous Materials*, vol. 141, no. 1, pp. 230–236, 2007.

[14] M. Huang, C. Xu, Z. Wu, Y. Huang, J. Lin, and J. Wu, "Photocatalytic discolorization of methyl orange solution by Pt modified $TiO_2$ loaded on natural zeolite," *Dyes and Pigments*, vol. 77, no. 2, pp. 327–334, 2008.

[15] B. Zhao, G. Mele, I. Pio, J. Li, L. Palmisano, and G. Vasapollo, "Degradation of 4-nitrophenol (4-NP) using Fe-$TiO_2$ as a heterogeneous photo-Fenton catalyst," *Journal of Hazardous Materials*, vol. 176, no. 1–3, pp. 569–574, 2010.

[16] J. Jing, J. Li, J. Feng, W. Li, and W. W. Yu, "Photodegradation of quinoline in water over magnetically separable $Fe_3O_4/TiO_2$ composite photocatalysts," *Chemical Engineering Journal*, vol. 219, pp. 355–360, 2013.

[17] R. Vinu, S. U. Akki, and G. Madras, "Investigation of dye functional group on the photocatalytic degradation of dyes by nano-$TiO_2$," *Journal of Hazardous Materials*, vol. 176, no. 1–3, pp. 765–773, 2010.

[18] H. R. Pouretedal, A. Norozi, M. H. Keshavarz, and A. Semnani, "Nanoparticles of zinc sulfide doped with manganese, nickel and copper as nanophotocatalyst in the degradation of organic dyes," *Journal of Hazardous Materials*, vol. 162, no. 2-3, pp. 674–681, 2009.

[19] T. T. Vu, L. del Río, T. Valdés-Solís, and G. Marbán, "Stainless steel wire mesh-supported ZnO for the catalytic photodegradation of methylene blue under ultraviolet irradiation," *Journal of Hazardous Materials*, vol. 246-247, pp. 126–134, 2013.

[20] R. Ullah and J. Dutta, "Photocatalytic degradation of organic dyes with manganese-doped ZnO nanoparticles," *Journal of Hazardous Materials*, vol. 156, no. 1–3, pp. 194–200, 2008.

[21] Y. Ju, J. Qiao, X. Peng et al., "Photodegradation of malachite green using UV-vis light from two microwave-powered electrodeless discharge lamps ($MPEDL_{-2}$): further investigation on products, dominant routes and mechanism," *Chemical Engineering Journal*, vol. 221, pp. 353–362, 2013.

[22] L. Shang, B. Li, W. Dong et al., "Heteronanostructure of Ag particle on titanate nanowire membrane with enhanced photocatalytic properties and bactericidal activities," *Journal of Hazardous Materials*, vol. 178, no. 1–3, pp. 1109–1114, 2010.

[23] R. Wahab, I. H. Hwang, Y.-S. Kim et al., "Non-hydrolytic synthesis and photo-catalytic studies of ZnO nanoparticles," *Chemical Engineering Journa*, vol. 175, pp. 450–457, 2011.

[24] K. Byrappa, A. K. Subramani, S. Ananda, K. M. L. Rai, R. Dinesh, and M. Yoshimura, "Photocatalytic degradation of rhodamine B dye using hydrothermally synthesized ZnO," *Bulletin of Materials Science*, vol. 29, no. 5, pp. 433–438, 2006.

[25] M. Soltaninezhad and A. Aminifar, "Study nanostructures of semiconductor zinc oxide (ZnO) as a photocatalyst for the degradation of organic pollutants," *International Journal of Nano Dimension*, vol. 2, no. 2, pp. 137–145, 2011.

[26] P. Sathishkumar, N. Pugazhenthiran, R. V. Mangalaraja, A. M. Asiri, and S. Anandan, "ZnO supported $CoFe_2O_4$ nanophotocatalysts for the mineralization of Direct Blue 71 in aqueous environments," *Journal of Hazardous Materials*, vol. 252-253, pp. 171–179, 2013.

[27] H. R. Rajabi, O. Khani, M. Shamsipur, and V. Vatanpour, "High-performance pure and $Fe^{3+}$-ion doped ZnS quantum dots as green nanophotocatalysts for the removal of malachite green under UV-light irradiation," *Journal of Hazardous Materials*, vol. 250-251, pp. 370–378, 2013.

[28] C. Shifu, Z. Wei, L. Wei, Z. Huaye, and Y. Xiaoling, "Preparation, characterization and activity evaluation of p-n junction photocatalyst p-$CaFe_2O_4$/n-ZnO," *Chemical Engineering Journal*, vol. 155, no. 1-2, pp. 466–473, 2009.

[29] X. Qiu, L. Li, J. Zheng, J. Liu, X. Sun, and G. Li, "Origin of the enhanced photocatalytic activities of semiconductors: a case study of ZnO doped with $Mg^{2+}$," *The Journal of Physical Chemistry C*, vol. 112, no. 32, pp. 12242–12248, 2008.

[30] N. Sobana and M. Swaminathan, "The effect of operational parameters on the photocatalytic degradation of acid red 18 by ZnO," *Separation and Purification Technology*, vol. 56, no. 1, pp. 101–107, 2007.

[31] H. Y. He, "Comparison study of photocatalytic properties of $SrTiO_3$ and $TiO_2$ powders in decomposition of methyl orange," *International Journal of Environmental Research*, vol. 3, no. 1, pp. 57–60, 2009.

[32] L. Karimi, S. Zohoori, and M. E. Yazdanshenas, "Photocatalytic degradation of azo dyes in aqueous solutions under UV irradiation using nano-strontium titanate as the nanophotocatalyst," *Journal of Saudi Chemical Society*, vol. 18, no. 5, pp. 581–588, 2014.

[33] H. Zhao, L. Liang, and H. wen Liu, "Fast photo-catalytic degradation of pyridine in nano aluminum oxide suspension systems," *Journal of Environmental Sciences*, vol. 23, supplement, pp. S156–S158, 2011.

[34] A. Di Paola, E. García-López, G. Marcì, and L. Palmisano, "A survey of photocatalytic materials for environmental remediation," *Journal of Hazardous Materials*, vol. 211-212, pp. 3–29, 2012.

[35] J. Saien, Z. Ojaghloo, A. R. Soleymani, and M. H. Rasoulifard, "Homogeneous and heterogeneous AOPs for rapid degradation of Triton X-100 in aqueous media via UV light, nano titania hydrogen peroxide and potassium persulfate," *Chemical Engineering Journal*, vol. 167, no. 1, pp. 172–182, 2011.

[36] T. Chen, Y. Zheng, J.-M. Lin, and G. Chen, "Study on the photocatalytic degradation of methyl orange in water using Ag/ZnO as catalyst by liquid chromatography electrospray ionization ion-trap mass spectrometry," *Journal of the American Society for Mass Spectrometry*, vol. 19, no. 7, pp. 997–1003, 2008.

[37] H. R. Pouretedal, M. H. Keshavarz, M. H. Yosefi, A. Shokrollahi, and A. Zali, "Photodegradation of HMX and RDX in the presence of nanocatalyst of zinc sulfide doped with copper," *Iranian Journal of Chemistry and Chemical Engineering*, vol. 28, no. 4, pp. 13–19, 2009.

[38] S. Chaturvedi, P. N. Dave, and N. K. Shah, "Applications of nano-catalyst in new era," *Journal of Saudi Chemical Society*, vol. 16, no. 3, pp. 307–325, 2012.

[39] N. A. M. Barakat, M. A. Kanjwal, I. S. Chronakis, and H. Y. Kim, "Influence of temperature on the photodegradation process using Ag-doped $TiO_2$ nanostructures: negative impact with the nanofibers," *Journal of Molecular Catalysis A: Chemical*, vol. 366, pp. 333–340, 2013.

[40] P. S. S. Kumar, M. R. Raj, and S. Anandan, "Nanoporous Au–TiMCM-41—an inorganic hybrid photocatalyst toward visible photooxidation of methyl orange," *Solar Energy Materials and Solar Cells*, vol. 94, no. 10, pp. 1783–1789, 2010.

[41] H. Y. He, J. F. Huang, L. Y. Cao, and J. P. Wu, "Photodegradation of methyl orange aqueous on $MnWO_4$ powder under different light resources and initial pH," *Desalination*, vol. 252, no. 1–3, pp. 66–70, 2010.

[42] J. Ananpattarachai, P. Kajitvichyanukul, and S. Seraphin, "Visible light absorption ability and photocatalytic oxidation activity of various interstitial N-doped $TiO_2$ prepared from different nitrogen dopants," *Journal of Hazardous Materials*, vol. 168, no. 1, pp. 253–261, 2009.

[43] M. A. Fox and M. T. Dulay, "Heterogeneous photocatalysis," *Chemical Reviews*, vol. 93, no. 1, pp. 341–357, 1993.

[44] Y. N. Tan, C. L. Wong, and A. R. Mohamed, "An overview on the photocatalytic activity of nano-doped-$TiO_2$ in the degradation of organic pollutants," *ISRN Materials Science*, vol. 2011, Article ID 261219, 18 pages, 2011.

[45] S. Ma, R. Li, C. Lv, W. Xu, and X. Gou, "Facile synthesis of ZnO nanorod arrays and hierarchical nanostructures for photocatalysis and gas sensor applications," *Journal of Hazardous Materials*, vol. 192, no. 2, pp. 730–740, 2011.

[46] Y. Liu, Y. Ohko, R. Zhang, Y. Yang, and Z. Zhang, "Degradation of malachite green on Pd/$WO_3$ photocatalysts under simulated solar light," *Journal of Hazardous Materials*, vol. 184, no. 1–3, pp. 386–391, 2010.

[47] M. M. Ba-Abbad, A. A. H. Kadhum, A. B. Mohamad, M. S. Takriff, and K. Sopian, "Synthesis and catalytic activity of $TiO_2$ nanoparticles for photochemical oxidation of concentrated chlorophenols under direct solar radiation," *International Journal of Electrochemical Science*, vol. 7, pp. 4871–4888, 2012.

[48] M. A. Barakat, H. Schaeffera, G. Hayes, and S. Ismat-Shah, "Photocatalytic degradation of 2-chlorophenol by Co-doped $TiO_2$ nanoparticles," *Applied Catalysis B: Environmental*, vol. 57, no. 1, pp. 23–30, 2005.

[49] F. D. Mai, C. S. Lu, C. W. Wu, C. H. Huang, J. Y. Chen, and C. C. Chen, "Mechanisms of photocatalytic degradation of Victoria Blue R using nano-$TiO_2$," *Separation and Purification Technology*, vol. 62, no. 2, pp. 423–436, 2008.

[50] N. Sobana, K. Selvam, and M. Swaminathan, "Optimization of photocatalytic degradation conditions of Direct Red 23 using nano-Ag doped $TiO_2$," *Separation and Purification Technology*, vol. 62, no. 3, pp. 648–653, 2008.

[51] S. Sakthivel, M. V. Shankar, M. Palanichamy, B. Arabindoo, D. W. Bahnemann, and V. Murugesan, "Enhancement of photocatalytic activity by metal deposition: characterisation and photonic efficiency of Pt, Au and Pd deposited on $TiO_2$ catalyst," *Water Research*, vol. 38, no. 13, pp. 3001–3008, 2004.

[52] V. Kruefu, H. Ninsonti, N. Wetchakun, B. Inceesungvorn, P. Pookmanee, and S. Phanichphant, "Photocatalytic degradation of phenol using Nb-loaded ZnO nanoparticles," *Engineering Journal*, vol. 16, no. 3, pp. 91–99, 2012.

[53] M. J. Pawar and V. B. Nimbalkar, "Synthesis and phenol degradation activity of Zn and Cr doped $TiO_2$ nanoparticles," *Research Journal of Chemical Sciences*, vol. 2, no. 1, pp. 32–37, 2012.

[54] V. Subramanian, E. E. Wolf, and P. V. Kamat, "Catalysis with $TiO_2$/gold nanocomposites. Effect of metal particle size on the fermi level equilibration," *Journal of the American Chemical Society*, vol. 126, no. 15, pp. 4943–4950, 2004.

[55] C. L. Yu, J. C. Yu, and M. Chan, "Sonochemical fabrication of fluorinated mesoporous titanium dioxide microspheres," *Journal of Solid State Chemistry*, vol. 182, no. 5, pp. 1061–1069, 2009.

[56] C.-H. Liang, M.-F. Hou, S.-G. Zhou et al., "The effect of erbium on the adsorption and photodegradation of orange I in aqueous $Er^{3+}$-$TiO_2$ suspension," *Journal of Hazardous Materials*, vol. 138, no. 3, pp. 471–478, 2006.

[57] M. A. Barakata, H. Schaeffera, G. Hayesa, and S. Ismat-Shaha, "Photocatalytic degradation of 2-chlorophenol by Co-doped $TiO_2$ nanoparticles," *Applied Catalysis B: Environmental*, vol. 57, no. 1, pp. 23–30, 2005.

[58] V. G. Gandhi, M. K. Mishra, M. S. Rao, A. Kumar, P. A. Joshi, and D. O. Shah, "Comparative study on nano-crystalline titanium dioxide catalyzed photocatalytic degradation of aromatic carboxylic acids in aqueous medium," *Journal of Industrial and Engineering Chemistry*, vol. 17, no. 2, pp. 331–339, 2011.

[59] M.-J. Gaoa, X.-D. Wanga, M. Guob, and M. Zhang, "Contrast on COD photo-degradation in coking wastewater catalyzed by $TiO_2$ and $TiO_2$-$TiO_2$ nanorod arrays," *Catalysis Today*, vol. 174, no. 1, pp. 79–87, 2011.

[60] B. Neppolian, S. R. Kanel, H. C. Choi, M. V. Shankar, B. Arabindoo, and V. Murugesan, "Photocatalytic degradation of reactive yellow 17 dye in aqueous solution in the presence of TiO2 with cement binder," *International Journal of Photoenergy*, vol. 5, no. 2, pp. 45–49, 2003.

[61] B. Neppolian, H. C. Choi, S. Sakthivel, B. Arabindoo, and V. Murugesan, "Solar/UV-induced photocatalytic degradation of three commercial textile dyes," *Journal of Hazardous Materials*, vol. 89, no. 2-3, pp. 303–317, 2002.

[62] N. Sobana, M. V. Muruganandam, and M. S. Swaminathan, "Characterization of AC–ZnO catalyst and its photocatalytic activity on 4-acetylphenol degradation," *Catalysis Communications*, vol. 9, no. 2, pp. 262–268, 2008.

[63] A. Zaleska, "Doped-$TiO_2$: a review," *Recent Patents on Engineering*, vol. 2, no. 3, pp. 157–164, 2008.

[64] J.-W. Shi, J.-T. Zheng, and P. Wu, "Preparation, characterization and photocatalytic activities of holmium-doped titanium dioxide nanoparticles," *Journal of Hazardous Materials*, vol. 161, no. 1, pp. 416–422, 2009.

[65] M. Kang, S.-J. Choung, and J. Y. Park, "Photocatalytic performance of nanometer-sized $Fe_xO_y$/$TiO_2$ particle synthesized by hydrothermal method," *Catalysis Today*, vol. 87, no. 1–4, pp. 87–97, 2003.

[66] J. Yu, H. Yu, B. Cheng, M. Zhou, and X. Zhao, "Enhanced photocatalytic activity of $TiO_2$ powder (P25) by hydrothermal treatment," *Journal of Molecular Catalysis A: Chemical*, vol. 253, no. 1-2, pp. 112–118, 2006.

[67] P. Sathishkumar, R. V. Mangalaraja, S. Anandan, and M. Ashokkumar, "$CoFe_2O_4$/$TiO_2$ nanocatalysts for the photocatalytic degradation of Reactive Red 120 in aqueous solutions in the presence and absence of electron acceptors," *Chemical Engineering Journal*, vol. 220, pp. 302–310, 2013.

[68] P. Fu, W. Lu, W. Lei, K. Wu, Y. Xu, and J. Wu, "Thermal stability and microstructure characterization of $MgAl_2O_4$ nanoparticles synthesized by reverse microemulsion method," *Materials Research*, vol. 16, no. 4, pp. 844–849, 2013.

[69] J. Fu, Y. Tian, B. Chang, F. Xi, and X. Dong, "Soft-chemical synthesis of mesoporous nitrogen-modified titania with superior photocatalytic performance under visible light irradiation," *Chemical Engineering Journal*, vol. 219, pp. 155–161, 2013.

[70] T. Soltani and M. H. Entezari, "Sono-synthesis of bismuth ferrite nanoparticles with high photocatalytic activity in degradation of Rhodamine B under solar light irradiation," *Chemical Engineering Journal*, vol. 223, pp. 145–154, 2013.

[71] F. Dong, W. Zhao, Z. Wu, and S. Guo, "Band structure and visible light photocatalytic activity of multi-type nitrogen doped $TiO_2$ nanoparticles prepared by thermal decomposition," *Journal of Hazardous Materials*, vol. 162, no. 2-3, pp. 763–770, 2009.

[72] A. Yousefi, A. Allahverdi, and P. Hejazi, "Effective dispersion of nano-$TiO_2$ powder for enhancement of photocatalytic properties in cement mixes," *Construction and Building Materials*, vol. 41, pp. 224–230, 2013.

[73] R. K. Upadhyay, M. Sharma, D. K. Singh, S. S. Amritphale, and N. Chandra, "Photo degradation of synthetic dyes using cadmium sulfide nanoparticles synthesized in the presence of different capping agents," *Separation and Purification Technology*, vol. 88, pp. 39–45, 2012.

[74] C. Chen, Z. Wang, S. Ruan, B. Zou, M. Zhao, and F. Wu, "Photocatalytic degradation of C.I. Acid Orange 52 in the presence of Zn-doped $TiO_2$ prepared by a stearic acid gel method," *Dyes and Pigments*, vol. 77, no. 1, pp. 204–209, 2008.

[75] J. Jing, J. Feng, W. Li, and W. W. Yu, "Low-temperature synthesis of water-dispersible anatase titanium dioxide nanoparticles for photocatalysis," *Journal of Colloid and Interface Science*, vol. 396, pp. 90–94, 2013.

[76] S. Song, Z. Sheng, Y. Liu, H. Wang, and Z. Wu, "Influences of pH value in deposition-precipitation synthesis process on Pt-doped

$TiO_2$ catalysts for photocatalytic oxidation of NO," *Journal of Environmental Sciences*, vol. 24, no. 8, pp. 1519–1524, 2012.

[77] S. Sohrabnezhad, A. Pourahmad, and E. Radaee, "Photocatalytic degradation of basic blue 9 by CoS nanoparticles supported on AlMCM-41 material as a catalyst," *Journal of Hazardous Materials*, vol. 170, no. 1, pp. 184–190, 2009.

[78] Y. Cao, Y. Cao, Y. Yu, P. Zhang, L. Zhang, and T. He, "An enhanced visible-light photocatalytic activity of $TiO_2$ by nitrogen and nickel-chlorine modification," *Separation and Purification Technology*, vol. 104, pp. 256–262, 2013.

[79] Y. Wu, M. Xing, B. Tian, J. Zhang, and F. Chen, "Preparation of nitrogen and fluorine co-doped mesoporous $TiO_2$ microsphere and photodegradation of acid orange 7 under visible light," *Chemical Engineering Journal*, vol. 162, no. 2, pp. 710–717, 2010.

[80] A. Fuerte, M. D. Hernández-Alonso, A. J. Maira et al., "Nanosize Ti-W mixed oxides: effect of doping level in the photocatalytic degradation of toluene using sunlight-type excitation," *Journal of Catalysis*, vol. 212, no. 1, pp. 1–9, 2002.

[81] R. Asahi, T. Morikawa, T. Ohwaki, K. Aoki, and Y. Taga, "Visible-light photocatalysis in nitrogen-doped titanium oxides," *Science*, vol. 293, no. 5528, pp. 269–271, 2001.

[82] V. Rodguez-Gonzalez, R. Zanella, G. del Angel, and R. Gomeza, "MTBE visible-light photocatalytic decomposition over Au/$TiO_2$ and Au/$TiO_2$–$Al_2O_3$ sol-gel prepared catalysts," *Journal of Molecular Catalysis A: Chemical*, vol. 281, no. 1-2, pp. 93–98, 2008.

[83] J.-L. Shie, C.-H. Lee, C.-S. Chiou, C.-T. Chang, C.-C. Chang, and C.-Y. Chang, "Photodegradation kinetics of formaldehyde using light sources of UVA, UVC and UVLED in the presence of composed silver titanium oxide photocatalyst," *Journal of Hazardous Materials*, vol. 155, no. 1-2, pp. 164–172, 2008.

[84] H.-Y. Lin, Y.-F. Chen, and Y.-W. Chen, "Water splitting reaction on NiO/$InVO_4$ under visible light irradiation," *International Journal of Hydrogen Energy*, vol. 32, no. 1, pp. 86–92, 2007.

[85] Q. Zhang, Q. Zhang, H. Wang, and Y. Li, "A high efficiency microreactor with Pt/ZnO nanorod arrays on the inner wall for photodegradation of phenol," *Journal of Hazardous Materials*, vol. 254-255, no. 1, pp. 318–324, 2013.

[86] A.-W. Xu, Y. Gao, and H.-Q. Liu, "The preparation, characterization, and their photocatalytic activities of rare-earth-doped $TiO_2$ nanoparticles," *Journal of Catalysis*, vol. 207, no. 2, pp. 151–157, 2002.

[87] T. Yu, X. Tan, L. Zhao, Y. Yin, P. Chen, and J. Wei, "Characterization, activity and kinetics of a visible light driven photocatalyst: cerium and nitrogen co-doped $TiO_2$ nanoparticles," *Chemical Engineering Journal*, vol. 157, no. 1, pp. 86–92, 2010.

[88] J. Xiao, T. Peng, R. Li, Z. Peng, and C. Yan, "Preparation, phase transformation and photocatalytic activities of cerium-doped mesoporous titania nanoparticles," *Journal of Solid State Chemistry*, vol. 179, no. 4, pp. 1161–1170, 2006.

[89] Y. Ma, J. Zhang, B. Tian, F. Chen, and L. Wang, "Synthesis and characterization of thermally stable Sm,N co-doped $TiO_2$ with highly visible light activity," *Journal of Hazardous Materials*, vol. 182, no. 1–3, pp. 386–393, 2010.

[90] T. Tong, J. Zhang, B. Tian, F. Chen, and D. He, "Preparation of $Fe^{3+}$-doped $TiO_2$ catalysts by controlled hydrolysis of titanium alkoxide and study on their photocatalytic activity for methyl orange degradation," *Journal of Hazardous Materials*, vol. 155, no. 3, pp. 572–579, 2008.

[91] H. Widiyandari, A. Purwanto, R. Balgis, T. Ogi, and K. Okuyama, "CuO/$WO_3$ and Pt/$WO_3$ nanocatalysts for efficient pollutant degradation using visible light irradiation," *Chemical Engineering Journal*, vol. 180, pp. 323–329, 2012.

[92] M. Ghaffari, H. Huang, P. Y. Tan, and O. K. Tan, "Synthesis and visible light photocatalytic properties of $SrTi_{(1-x)}Fe_xO_{(3-\sigma)}$ powder for indoor decontamination," *Powder Technology*, vol. 225, pp. 221–226, 2012.

[93] T. Morikawa, R. Asahi, T. Ohwaki, K. Aoki, K. Suzuki, and Y. Taga, "Visible-light photocatalyst—nitrogen doped titanium dioxide," *R&D Review of Toyota CRDL*, vol. 40, no. 3, pp. 45–50, 2005.

[94] S. Sakthivel and H. Kisch, "Daylight photocatalysis by carbon-modified titanium dioxide," *Angewandte Chemie International Edition*, vol. 42, no. 40, pp. 4908–4911, 2003.

[95] H. Wang and J. P. Lewis, "Effects of dopant states on photoactivity in carbon-doped $TiO_2$," *Journal of Physics: Condensed Matter*, vol. 17, no. 21, 2005.

[96] J. C. Yu, J. Yu, W. Ho, Z. Jiang, and L. Zhang, "Effects of $F^-$ doping on the photocatalytic activity and microstructures of nanocrystalline $TiO_2$ powders," *Chemistry of Materials*, vol. 14, no. 9, pp. 3808–3816, 2002.

[97] T. Tong, J. Zhang, B. Tian, F. Chen, D. He, and M. Anpo, "Preparation of Ce–$TiO_2$ catalysts by controlled hydrolysis of titanium alkoxide based on esterification reaction and study on its photocatalytic activity," *Journal of Colloid and Interface Science*, vol. 315, no. 1, pp. 382–388, 2007.

[98] Z. Xu, Q. Yang, C. Xie et al., "Structure, luminescence properties and photocatalytic activity of europium doped-$TiO_2$ nanoparticles," *Journal of Materials Science*, vol. 40, no. 6, pp. 1539–1541, 2005.

[99] X. Zhang, F. Wu, X. Wu, P. Chen, and N. Deng, "Photodegradation of acetaminophen in $TiO_2$ suspended solution," *Journal of Hazardous Materials*, vol. 157, no. 2-3, pp. 300–307, 2008.

[100] H. Seshadri, S. Chitra, K. Paramasivan, and P. K. Sinha, "Photocatalytic degradation of liquid waste containing EDTA," *Desalination*, vol. 232, no. 1–3, pp. 139–144, 2008.

[101] N. Venkatachalam, M. Palanichamy, B. Arabindoo, and V. Murugesan, "Enhanced photocatalytic degradation of 4-chlorophenol by $Zr^{4+}$ doped nano $TiO_2$," *Journal of Molecular Catalysis A: Chemical*, vol. 266, no. 1-2, pp. 158–165, 2007.

[102] J. Zhang, T. Ayusawa, M. Minagawa et al., "Investigations of $TiO_2$ photocatalysts for the decomposition of NO in the flow system: the role of pretreatment and reaction conditions in the photocatalytic efficiency," *Journal of Catalysis*, vol. 198, no. 1, pp. 1–8, 2001.

[103] H. Sun, Y. Bai, W. Jin, and N. Xu, "Visible-light-driven $TiO_2$ catalysts doped with low-concentration nitrogen species," *Solar Energy Materials and Solar Cells*, vol. 92, no. 1, pp. 76–83, 2008.

[104] F. Li, S. Sun, Y. Jiang, M. Xia, M. Sun, and B. Xue, "Photodegradation of an azo dye using immobilized nanoparticles of $TiO_2$ supported by natural porous mineral," *Journal of Hazardous Materials*, vol. 152, no. 3, pp. 1037–1044, 2008.

[105] Y.-J. Chiang and C.-C. Lin, "Photocatalytic decolorization of methylene blue in aqueous solutions using coupled ZnO/$SnO_2$ photocatalysts," *Powder Technology*, vol. 246, pp. 137–143, 2013.

[106] C. Karunakaran and R. Dhanalakshmi, "Semiconductor-catalyzed degradation of phenols with sunlight," *Solar Energy Materials and Solar Cells*, vol. 92, no. 11, pp. 1315–1321, 2008.

[107] A. G. S. Prado and L. L. Costa, "Photocatalytic decouloration of malachite green dye by application of $TiO_2$ nanotubes," *Journal of Hazardous Materials*, vol. 169, no. 1–3, pp. 297–301, 2009.

[108] N. Sapawe, A. A. Jalil, and S. Triwahyono, "Photodecolorization of methylene blue over $EGZrO_2$/EGZnO/$EGFe_2O_3$/HY photocatalyst: effect of radical scavenger," *Malaysian Journal of Fundamental and Applied Sciences*, vol. 9, no. 2, pp. 67–73, 2013.

[109] T. A. Saleh, M. A. Gondal, Q. A. Drmosh, Z. H. Yamani, and A. AL-yamani, "Enhancement in photocatalytic activity for acetaldehyde removal by embedding ZnO nano particles on multiwall carbon nanotubes," *Chemical Engineering Journal*, vol. 166, no. 1, pp. 407–412, 2011.

[110] X. Qiu, Z. Fang, B. Liang, F. Gu, and Z. Xu, "Degradation of decabromodiphenyl ether by nano zero-valent iron immobilized in mesoporous silica microspheres," *Journal of Hazardous Materials*, vol. 193, pp. 70–81, 2011.

[111] M. S. Lucas, P. B. Tavares, J. A. Peres et al., "Photocatalytic degradation of Reactive Black 5 with $TiO_2$-coated magnetic nanoparticles," *Catalysis Today*, vol. 209, pp. 116–121, 2013.

[112] R. Shao, L. Sun, L. Tang, and Z. Chen, "Preparation and characterization of magnetic core-shell $ZnFe_2O_4$@ZnO nanoparticles and their application for the photodegradation of methylene blue," *Chemical Engineering Journal*, vol. 217, pp. 185–191, 2013.

[113] S. Liu, H. Sun, S. Liu, and S. Wang, "Graphene facilitated visible light photodegradation of methylene blue over titanium dioxide photocatalysts," *Chemical Engineering Journal*, vol. 214, pp. 298–303, 2013.